Sergi, C., Sarasini, F., Russo, P., Vitiello, L., Barbero, E., Sanchez-Saez, S. & Tirillò, J. (2022). Experimental and numerical analysis of the ballistic response of agglomerated cork and its bio-based sandwich structures. *Engineering Failure Analysis, 131*, 105904.

DOI: 10.1016/j.engfailanal.2021.105904

EXPERIMENTAL AND NUMERICAL ANALYSIS OF THE BALLISTIC RESPONSE OF AGGLOMERATED CORK AND ITS BIO-BASED SANDWICH STRUCTURES

Claudia Sergi[1,2*], Fabrizio Sarasini[1], Pietro Russo[3], Libera Vitiello[4], Enrique Barbero[2], Sonia Sanchez-Saez[2], Jacopo Tirillò[1]

[1] Department of Chemical Engineering Materials Environment, Sapienza Università di Roma and UdR INSTM, Italy

[2] Department of Continuum Mechanics and Structural Analysis, Universidad Carlos III de Madrid, Spain

[3] Institute for Polymers, Composites and Biomaterials, National Research Council, Pozzuoli, Naples, Italy

[4] Department of Chemical, Materials and Production Engineering, University of Naples Federico II, Italy

*Corresponding author: claudia.sergi@uniroma1.it

ABSTRACT

Considering the susceptibility of sandwich structures to impact events and the increasing environmental awareness due to pollution, the present work provides a thorough understanding of the ballistic impact behavior of agglomerated cork and of the resulting green sandwich structures produced with polypropylene (PP) skins reinforced with a flax/basalt intraply hybrid fabric. The effect of density on the agglomerated cork response was evaluated (NL10 ρ=0.14 g/cm^3, NL20 ρ=0.20 g/cm^3 and NL25 ρ=0.25 g/cm^3) and a comparison with commercial polyvinyl(chloride) foams was provided (HP130 ρ=0.13 g/cm^3, HP200 ρ=0.20 g/cm^3 and HP250 ρ=0.25 g/cm^3). The effect of a maleic anhydride coupling agent on the mechanical properties of the skins and of the overall sandwich structures was also investigated. The results highlighted a compromising effect of the weak interface between cork granules and polymeric binder on the impact resistance of the agglomerated cork, but a clear improvement of its performance was observed when embedded as core material between the two skins. Indeed, the two classes of sandwich structures produced with neat PP skins and with the two cores with the same density, i.e. agglomerated cork NL10 and PVC foam HP130, displayed the same ballistic limit of 171 m/s confirming that cork integration in the overall structures allows to approach PVC foam performance. The high-velocity impact response of one agglomerated cork (NL25) and one PVC foam (HP130) was also subjected to finite element analysis employing the CRUSHABLE FOAM model available in ABAQUS obtaining a good fitting with the experimental data.

Keywords: Agglomerated Cork, PVC foam, Basalt, Flax, Ballistic Impact

1 INTRODUCTION

Ballistic impacts are usually associated with impact shielding materials such as Kevlar [1] and ultra-high-molecular-weight polyethylene (UHMWPE) [2] expressly designed to offer protection against projectile and bullets in armed conflicts or to preserve the integrity of structures, such as aerospace ones, from debris. Besides this specific research field, it must be considered that high-velocity impact events can occur in everyday life involving structures which are not specifically designed for shielding purposes and which can suffer a severe decay in the mechanical properties and the structural performance. Polymer composite materials are widespread in most industrial fields such as automotive, marine and aerospace where the guarantee of structure reliability and integrity against impact is of main importance. For this reason, many studies addressed the ballistic impact resistance of composite laminates and in particular the one of glass fiber composites [3,4], which are the most extensively used.

Sandwich structures are another class of composite materials which are negatively affected by impact events and whose consequent drop in the mechanical properties needs to be carefully studied and controlled. In light of this, many research works focused on the ballistic impact behavior of both foam core and honeycomb core sandwich panels. The ballistic response of sandwich structures with glass fiber reinforced skins and polymeric foam core was investigated from different points of view, i.e. experimental [5], numerical [6] and analytical [7]. Another class of sandwich structures with foam core which was largely subjected to ballistic analysis is the one of aluminum face-sheet composites whose feasibility was assessed for both marine [8] and aerospace [9] applications. Concerning sandwich panels with honeycomb cores, Aryal et al. [10] investigated the residual structural properties of ballistic impacted carbon fiber skins and Nomex honeycomb sandwich composites which experienced a reduction between 34 % and 55 % of their compression properties, whereas Wang et al. [11] investigated the effect of honeycomb design on the overall structure ballistic response and found out that circular honeycomb in square and hexagonal arrangement are able to improve of 15.2 % and 25 % the ballistic limit of the structure with respect to hexagonal honeycombs.

The increasing environmental awareness encouraged the exploitation of natural materials from renewable resources in the production of more sustainable composites and endorsed the assessment of their feasibility in replacement of synthetic and petroleum-based ones. In light of this and in consideration of the likelihood of ballistic strikes and impacts, some studies focused on the ballistic behavior of bio-based composites and sandwich structures. Santos da Luz et al. [12] compared the ballistic performance of an epoxy resin reinforced with pineapple leaf fibers with the ones of UHMWPE backing the front ceramic of multilayered armor systems. They found out that the green composite is able to decrease the back-face signature to 26.6 mm, which is significantly lower than 41.5 mm achievable with UHMWPE. Moving to environmentally friendly sandwich structures, Jover et al. [13] investigated the damage induced by single and multiple high velocity impacts on carbon fibers and balsa wood core sandwich structures disclosing a ballistic limit of 96 m/s which allowed their implementation for shielding against debris resulting from blast and tornado.

Another natural and biodegradable core which aroused great interest thanks to its excellent energy absorbing and damping capabilities, resulting from its peculiar morphology, i.e. cell-walls undulation, is agglomerated cork. Thanks to these appealing features which make it suitable for energy absorbing devices such as helmets, many research studies addressed its impact response in compressive conditions [14–16], as a function of temperature [17–19] and number of impacts [20], and its low velocity impact response when employed as core materials in sandwich structures [21–24]. Only few studies are available on the ballistic impact response of agglomerated cork sandwich structures like the ones proposed by Sanchez-Saez et al. [25], who investigated a face-sheeted aluminum structure, by Sarasini et al. [26] who studied a green sandwich composite with flax fibers reinforced skins and by Ivañez et al. [27] who assessed the high-velocity impact response of pre-damaged carbon/epoxy sandwich panels.

In consideration of the low amount of information available on agglomerated cork sandwich structure response to ballistic impacts, the present work aims to bridge this gap of knowledge addressing the high-velocity impact response of agglomerated cork and of its almost full bio-based sandwich structures produced with polypropylene skins reinforced with a natural flax/basalt hybrid woven fabric. Three agglomerated corks with different densities were selected to investigate the effect of this parameter on the ballistic limit of the cores and of the overall structures and the results were compared with the ones of three well-established closed-cell PVC foams, characterized by the same densities of the green cores selected, employed as benchmark. Concerning the skins, the effect of a maleic anhydride coupling agent on the impact response of the laminates and of the whole sandwich panels was evaluated. To complement the extensive experimental campaign, a finite element analysis (FEA) of the high-velocity impact response of the denser cork (NL25) and of the polymeric foam with the closest performance, i.e. HP130, was carried out with the software ABAQUS. The analysis was performed using the CRUSHABLE FOAM material model available in the program and turned out to be a good support to the valid numerical analysis already proposed by Fernandes et al. [28]. In their study, they focused on the impact response of cork in compression employing the hyper-elastic model and the Mullins effect to model material damage at high deformations, but neglecting the perforation phenomena that can occur in different impact conditions such as puncture and ballistic impacts. The present work proposes a possible solution to simulate the perforation phenomena which may involve cork and the related sandwich structures. In view of this, the cores rather than the complete sandwich structures were numerically modelled to provide a tool efficient not only for the present work purposes, but also for other sandwich configurations.

2 MATERIALS AND METHODS

2.1 Materials

The ballistic impact campaign was carried out on the complete sandwich structures, but also on the cores and skins to investigate their response and the evolution of their behavior resulting from their assembly. Six core materials were selected for the core testing phase, i.e. three agglomerated corks with different densities and three PVC foams with the same densities of the bio-based cores. The selection of different core densities allowed to disclose the effect of this parameter on the ballistic limit while the employment of the polymeric foams as baseline allowed to point out the differences with the natural cores response. NL10 (0.14 g/cm^3), NL20 (0.20 g/cm^3) and NL25 (0.25 g/cm^3) in the form of 15 mm-thick planks, were provided by Amorim Cork Composites® while PVC closed cells foams, commercially known as Divinycell HP130 (0.13 g/cm^3), Divinycell HP200 (0.20 g/cm^3) and Divinycell HP250 (0.25 g/cm^3), were provided by Diab®.

Thermoplastic polypropylene skins reinforced with a LINCORE® HF T2 360 intraply flax/basalt hybrid fabric, provided by Depestele Group, and produced by hot compression molding (P400E by Collin GmbH) were selected. The influence of a maleic anhydride grafted polypropylene (MA-g-PP) added to the neat matrix was also evaluated. The neat PP matrix, Bormod™ HF955MO, was supplied by Borealis AG and the MA-g-PP Polybond® 3000 with a maleic anhydride content of 1.2 wt% was supplied by Chemtura. The compatibilized skins (PPC) were produced by adding 2 wt% of coupling agent to the neat polypropylene (PP) by means of a corotating twin screw extruder Collin Teach-Line® ZK25T operating with a temperature profile of 180 °C - 190 °C - 205 °C - 195 °C -185 °C and a 60 rpm screw speed. To perform hot compression, the polymeric matrix was provided in the form of films (thickness 35-40 µm) obtained with a film blowing extrusion line Teach-Line® E 20 T by Collin GmbH equipped with a calender CR72T. The apparatus operated with a screw speed of 55 rpm and a temperature profile of 180 °C - 190 °C - 200 °C - 190 °C -185 °C. The reinforcement fabric is a balanced twill 2/2 fabric made up with 50 wt% of basalt and 50 wt% of flax and with an areal density of 360 g/m^2. Skins were produced by alternating a film of matrix and a ply of fabric for a total number of four twill layers according to the optimized manufacturing process shown in Figure S1 of Supplementary Materials.

Based upon the results obtained on cores, two agglomerated corks, i.e. NL10 and NL25, and one foam, i.e. HP130, were selected as core material to produce the sandwich structures with both PP and PPC skins. NL10 and HP130 cores provide a direct comparison of structures with the same weight and the use of NL25 and HP130 enables the comparison of the cork and the foam with the closest mechanical behavior. The bicomponent epoxy resin Elan-tech® ADH 46.46 by Elantas was employed to bond together core and skins. Polypropylene is a low surface energy polyolefin and provides a poor adhesion with the structural adhesives commercially available hence skins first polymeric layer was removed with a coarse-grained sandpaper to improve interfacial adhesion between core and skins. A two-step process was used to produce sandwich structures. After gluing the first skin, 24 hours were allowed before gluing the second one to ensure resin complete curing. The structure was subjected to a constant load during curing to promote interfacial adhesion and in every step the glued skin was placed below the core to avoid resin gravity-driven percolation in the core.

2.2 Ballistic Impact

Ballistic impact tests were performed on square samples with 100 mm of side employing a gas gun, shown in Figure 1, fed with a gas blend of Ar and CO_2 for the lower impact velocities and with helium at high pressure for the higher impact velocities. A steel spherical projectile with a 7.5 mm diameter and a 1.7 g weight was employed. All impacts were recorded with the Fastcam SA-Z high-speed camera by Photron® and the resulting videos were processed with the program Photron FASTCAM Viewer 3 to compute the impact velocity, V_{imp}, and the residual velocity, V_{res}, of the projectile.

At least 15 samples were impacted for each core, skin and sandwich type and the resulting impact and residual velocities data sets were plotted to estimate the ballistic limit applying the Lambert-Jonas correlation [29]:

$$V_{res} = a(V_{imp}^2 - V_{bl}^2)^{\frac{1}{2}} \tag{1}$$

where V_{imp} and V_{res} are obtained by test videos processing and a and V_{bl}, i.e. the ballistic limit, are two unknown parameters which can be calculated through the least square method, i.e. an error minimization process.

Figure 1: Gas gun and projectile used to perform ballistic impact tests

A post-impact analysis was also carried out on core specimens through the image processing program Image J to evaluate the damage area extent as a function of impact velocity. The analysis was performed on the photographs of the damaged samples which were converted in black and white images and were subjected to a thresholding process, i.e. an image segmentation that converts a grayscale image in a binary image. This technique is largely employed to highlight and select areas of interest thus allowing to identify the damage area that, once highlighted and confined, can be measured automatically by the program.

2.3 Core materials Finite Element analysis: the model

Based upon the results obtained on the cores, it appeared evident that NL25 agglomerated cork and HP130 PVC foams are the core with the closest ballistic response and for this reason were selected to carry out the finite element analysis with the software ABAQUS. The feasibility of the CRUSHABLE FOAM material model to reproduce the high-velocity impact behavior of the cores under study was initially assessed applying such model to the synthetic foam and, only once validated, to the natural core which is characterized by a more complex and heterogeneous response.

In light of the symmetry of the problem under study, only a quarter of the geometry of both sample and projectile was modelled in order to reduce the computational time as shown in Figure 2. Concerning the boundary conditions (Figure 2.a) of the target, the upper side of the specimen was provided with a fixed boundary condition which constrains all the degrees of freedom of the region whereas the right side and the lower side of the specimen were provided with a X-symmetric and Y-symmetric boundary condition, respectively, which allows to account for the problem symmetry. Concerning the projectile, all its degrees of freedom were constrained except for the displacement along the z-axis, i.e. the impact direction. Moving to the material modelling, the projectile is made of steel hence it was simulated with a linear elastic material model with a density of 7.7 g/cm^3, a Poisson's ratio of 0.3 and an elastic modulus of 210 GPa. More complex is the model employed to simulate the impact response of HP130 foam, in fact it was necessary to split its behavior and to define separately the elastic region, the plasticity zone and the damage initiation and evolution criterion.

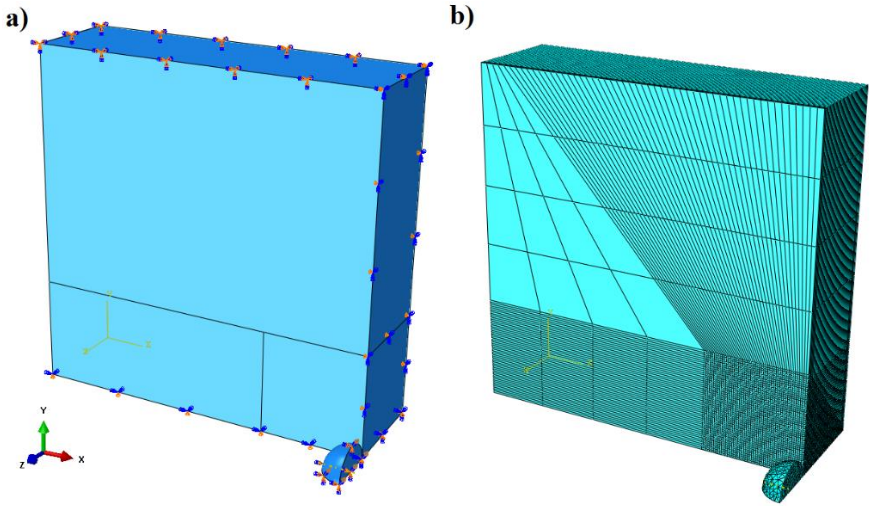

Figure 2: Quarter model employed to carry out the finite element analysis: boundary conditions (a) and mesh distribution (b)

The elastic region was modelled as a linear elastic region defining a density of 0.13 g/cm^3 and a Poisson's ratio of 0.4, according to the data provided by the supplier, and an elastic modulus of 70 MPa according to the data collected during a preliminary quasi-static experimental campaign. The plastic behavior of the foam was described through the CRUSHABLE FOAM material model selecting the volumetric option as proposed by Carranza et al. [30]. This option requires the definition of the compressive yield stress ratio, Kc, and the hydrostatic yield stress ratio, Kt, which are defined as the ratio of initial yield stress in uniaxial compression, σ_{c0}, to initial yield stress in hydrostatic compression, p_c, and the ratio of yield stress in hydrostatic tension, p_t, to initial yield stress in hydrostatic compression, respectively. Considering that hydrostatic test data are difficult to collect and to find in literature, an alternative path was followed to identify Kc and Kt values. In their work, Carranza et al. defined the elliptical yield surface of the crushable foam material model starting from the uniaxial tensile yield stress, σ_{t0}, uniaxial compression yield stress, σ_{c0}, and the shear strength, τ_0. The same procedure was applied in this work taking advantage of the data collected during the preliminary quasi-static experimental campaign and the resulting elliptical yield surface of HP130 is shown in Figure 3. Once inferred p_t and p_c, Kc and Kt values were calculated and set equal to 1.667 and 2.886, respectively. The CRUSHABLE FOAM material model also requires the evolution of the yield stress as a function of the equivalent plastic strain. Even in this case the quasi-static experimental data were employed and the curve provided to the program is shown in Figure S2 of Supplementary Materials. Finally, the damage criterion was entered in the model and the ductile damage was employed in the finite element analysis setting a fracture strain of 1.8 in the damage initiation and a displacement of 0.1 mm in damage evolution.

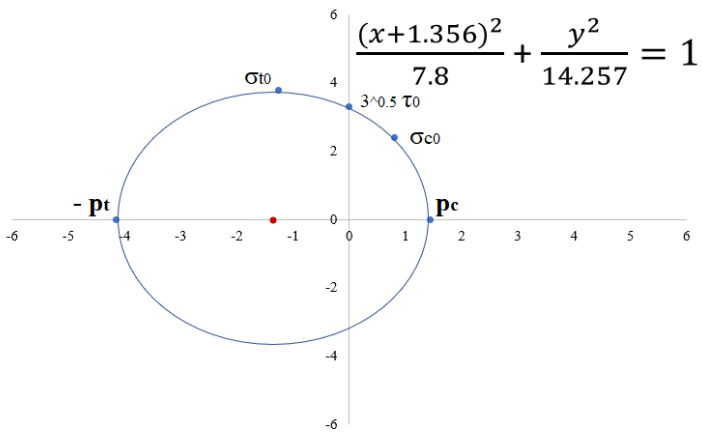

Figure 3: Yield surface of HP130 employed to calculate p_t and p_c

The interaction between the projectile and the sample was modelled as a hard contact in the normal behavior and with a friction coefficient of 0.3 in the tangential behavior. The friction coefficient value was selected as the average value of the friction coefficients employed in different studies on various thermoplastic foams [30–

32]. Concerning the mesh, the projectile was discretized with 10-node modified quadratic tetrahedron elements (C3D10M) with 0.7 mm of size which is the highest dimension able to provide convergence of the results. The impacted sample was meshed with 8-node linear brick elements (C3D8R) with hourglass control employing a refined mesh of 0.3 mm near the impacted zone (Figure 2.b) in order to provide accurate results without increasing excessively the computational time. The selected mesh size is the best compromise between solution convergence and computational time (CPU time) as also proved by the data reported in Figure S3 of Supplementary Materials where the green points represent the conditions selected for the present work.

In light of the good results obtained on the PVC foam, the same configuration of the problem was employed to carry out the analysis on NL25 agglomerated cork changing the material model parameters. The elastic region was modelled defining a density of 0.25 g/cm^3 and, according to the data provided by the supplier, a Poisson's ratio of 0 [33] and an elastic modulus of 22 MPa according to the data collected during the preliminary quasi-static experimental campaign. The CRUSHABLE FOAM material model was again selected to model the plastic behavior of the core, but in this case the isotropic option was selected considering unsatisfying the results obtained with the volumetric option. This could be explained considering the results reported by Tita et al. [34] who found out that the volumetric model performs worse than the isotropic one in tension based model. The isotropic model is more feasible when modelling multi-axial loads where tension, shear and compression stresses are comparable. As it will be shown later in the experimental results, shear and tensile loads play a major role in agglomerated cork impact response determining the cork granules-polymeric binder failure preventing the full exploitation of cork energy absorption capabilities and making tensile and shear loads as important as compressive ones. Moving back to the CRUSHABLE FOAM model, even in this case the material model requires again the compressive yield stress ratio, Kc, which was calculated and sets equal to 2, and the plastic Poisson's ratio that was set equal to 0.05 according to the data provided by Jardin et al. [15]. Even in this case the evolution of the yield stress as a function of the equivalent plastic strain needs to be provided to the software and the employed curve is reported in Figure S2 of Supplementary Materials. A fracture strain of 0.85 was entered in the ductile damage criterion as damage initiation and a displacement of 0.1 mm was introduced in damage evolution. Another difference with the synthetic foam simulation lies in the addition of distortion control to the C3D8R elements, employed to mesh the sample, to improve solution accuracy. Moreover, solution mesh independency is already achieved for a 0.5 mm element size in agglomerated cork (Figure S4 of Supplementary Materials) therefore these are the dimensions selected to carry out the natural core analysis to further reduce the CPU time. All material model coefficients for both PVC foam and agglomerated cork are summarized in Table 1.

Table 1: Ballistic limits of the six sandwich structures under study

PVC Foam HP130		**Agglomerated Cork NL25**	
Parameter	**Value**	**Parameter**	**Value**
Elastic Region			
Density (g/cm^3)	0.13	Density (g/cm^3)	0.25
Poisson's ratio	0.4	Poisson's ratio	0
Elastic Modulus (MPa)	70	Elastic Modulus (MPa)	22
Plateau Region			
Volumetric Hardening		Isotropic Hardening	
Kc	1.667	Kc	0.2
Kt	2.886	Plastic Poisson's ratio	0.05
Fracture			
Fracture Strain	1.8	Fracture Strain	0.85
Displacement at failure (mm)	0.1	Displacement at failure (mm)	0.1

3 RESULTS AND DISCUSSION

3.1 Core Ballistic Response

Figure 4 shows the experimental data (red dots) of projectile residual velocity as a function of impact velocity, for all agglomerated corks and PVC foams, employed to identify the ballistic limit of the core materials applying the Lambert-Jonas interpolation (blue line) using a least square fitting. The resulting ballistic limit values as a function of core density are summarized in Figure 5. All PVC foams are characterized by a higher ballistic resistance than all agglomerated corks regardless of the density and this can be ascribed to the higher intrinsic strength of the synthetic cores, but also to the premature detachment of agglomerated cork plugs due to the poor interface between cork granules and the polyurethane binder which prevents the full exploitation of cork energy absorbing capacities. Both core types exhibit an increase in the ballistic limit with increasing density, but the trend that describes this increment is completely different, in fact PVC foams experiences a linear increase of the ballistic limit with density ($R^2 = 0.996$) whereas agglomerated corks display an increase in the ballistic limit characterized by a decreasing rate. This is consistent with the different chemical composition and microstructure of the cores under study. An increase in PVC foams density is due to a lower air content and hence to thicker cell walls thus implying a higher amount of energy to dissipate before reaching perforation. Concerning agglomerated cork, core density increase must be ascribed to a higher compactness of the granules and not to a change in cell walls microstructure. Moreover, its main point of weakness, i.e. polymeric binder-cork granules interface, is responsible for the premature intergranular fracture of the material thus acting as a bottle neck that delimits the upper limit achievable with the bio-based cores.

The features that determine the differences in core ballistic limit trends are also useful to explain the different damage mode observed in the two types of core. Figure 6 shows the common plugging damage mode observed in PVC foams whereas Figure 7 reports the typical conical intergranular fracture that occurs in agglomerated cork samples. The plugging damage mode of the rigid PVC foams is characterized by a cylindrical shape and can be ascribed to a strong localization of the impact which determines an excessive localized plasticity. Considering that all chemical bonds in PVC backbone are characterized by the same strength, it appears evident that the cylindrical rupture is the less energy consumption path for crack propagation. Completely different is agglomerated cork damage which consists of a conoid intergranular fracture, which initiates in the area impacted by the projectile and propagates throughout sample thickness. This type of fracture can be attributed to two main factors. The first one is the already mentioned weak granules-binder interface which acts as a preferential path for crack propagation being the less energy consuming. This means that the crack changes its path every time that encounters a cork granule thus leading to a progressive enlargement of the detached area. The second reason can be found in the low solid mass volume fraction, approximately 10 %, which characterizes natural cork as reported by Pereira [35] and which will increases slightly for agglomerated cork due to the presence of the polymeric binder. This means that cork granules interfaces can be recognized as the areas where material mass concentrates thus acting as a preferential path for shock wave propagation.

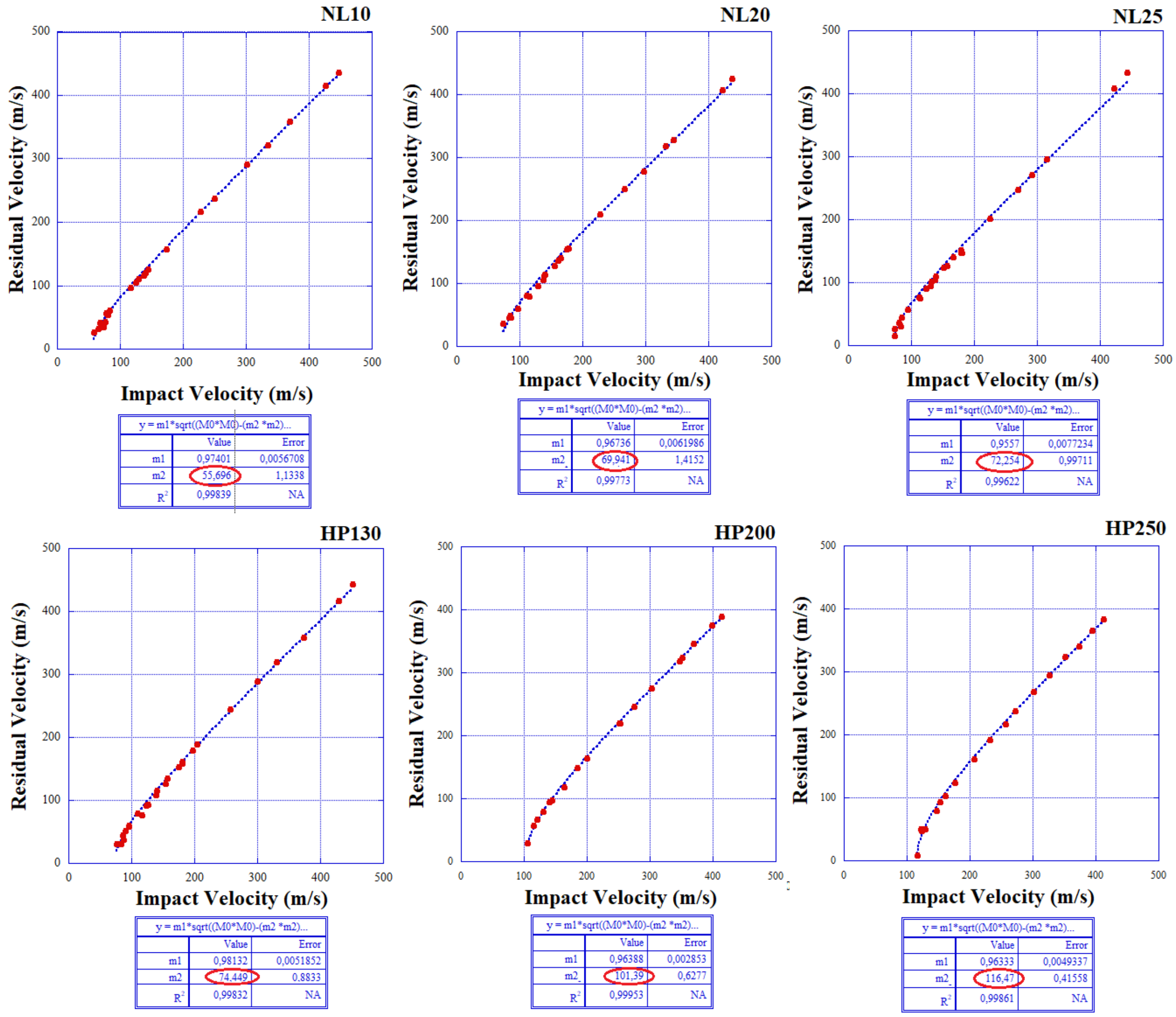

Figure 4: Agglomerated cork (NL10, NL20 and NL25) and PVC foams (HP130, HP200 and HP250) experimental data (red dots) and interpolation curves (blue line) obtained implementing the Lambert-Jonas equation through a least square method

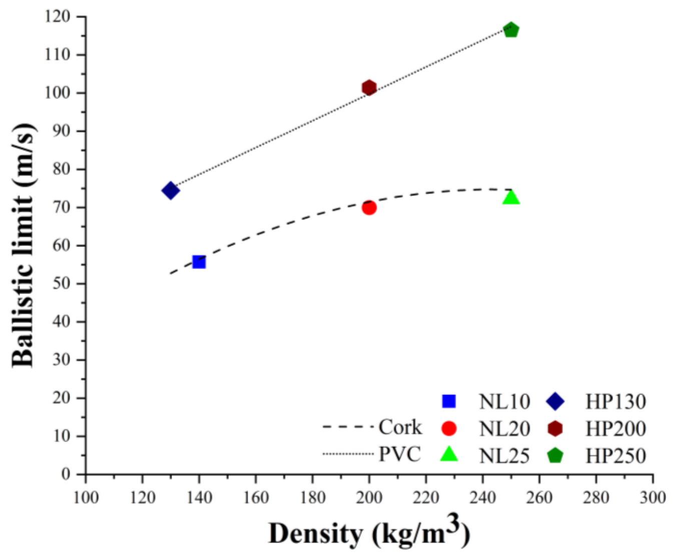

Figure 5: Ballistic limits of the six core materials calculated through the Lambert-Jonas equation as a function of core density

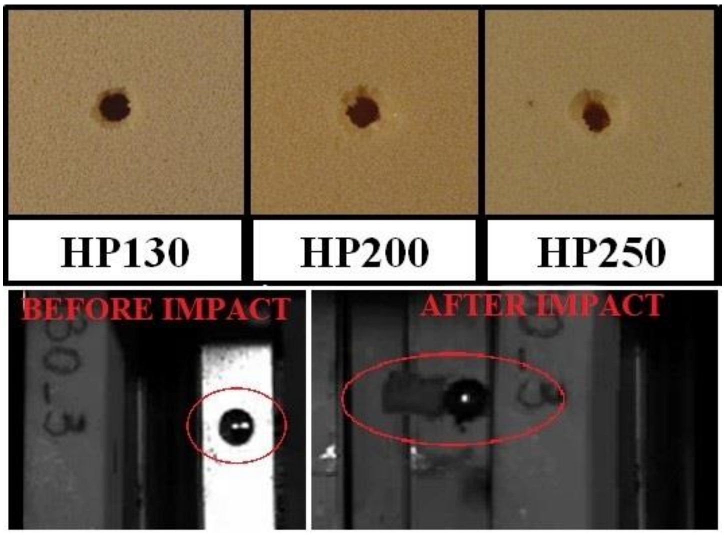

Figure 6: Plugging damage mode typical of PVC foams and 110 m/s impact progression of a HP130 foam

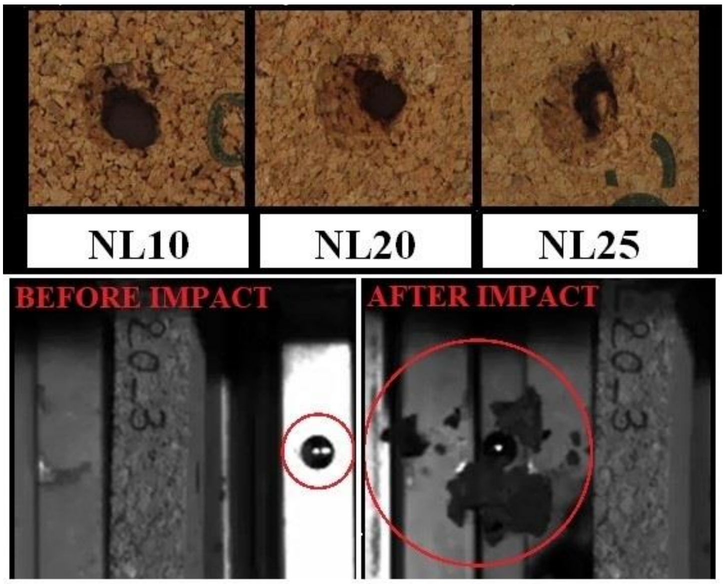

Figure 7: Conical intergranular fracture typical of agglomerated corks and 84 m/s impact progression of a NL20 agglomerated cork

Core damage was further investigated through the program Image J, which allowed to evaluate the extent of the damage area as a function of impact velocity, and the resulting values are reported in Figure 8. All cores, regardless of their nature and density, display a decrease in back damage area for increasing impact velocities and this is coherent with the results presented by Buitrago et al. [36], by López-Puente et al.[37] and by Amaro et al [38] who found out a similar trend for glass/polyester, carbon/epoxy and Kevlar/cork powder/epoxy composites, respectively. This response, which has been reported in materials of very different nature, must be ascribed to the very short interaction time between the sample and the projectile during a high-velocity impact. Indeed, the closer the material to its ballistic limit the higher the material reaction time and hence the amount of sample interested by the impact which results in a lower damage localization. In the present work, agglomerated corks display a reduction in back damage extent between 72.2 % and 88.4 % and PVC foams between 92 % and 96 % moving along the whole impact velocity range. Moreover, all cores are characterized by a lower threshold value of back damage extent which is around 90 mm^2 for agglomerated corks and 10 mm^2 for PVC foams. Considering that the projectile is characterized by a 7.5 mm diameter, its cross section is of 44.16 mm^2 meaning that the back damage area threshold of cork is two times higher than projectile dimension. Despite its unique dimensional recovery capabilities, agglomerated cork experiences such a wide damage extent due to the conical propagation of the fracture across the polymeric binder. Different is the situation for the PVC foams characterized by a damage threshold 77.3 % lower with respect to projectile dimension. This can be ascribed to the high elastic deformation in compression experienced by the cylindrical hole which is recovered once the projectile leaves the sample.

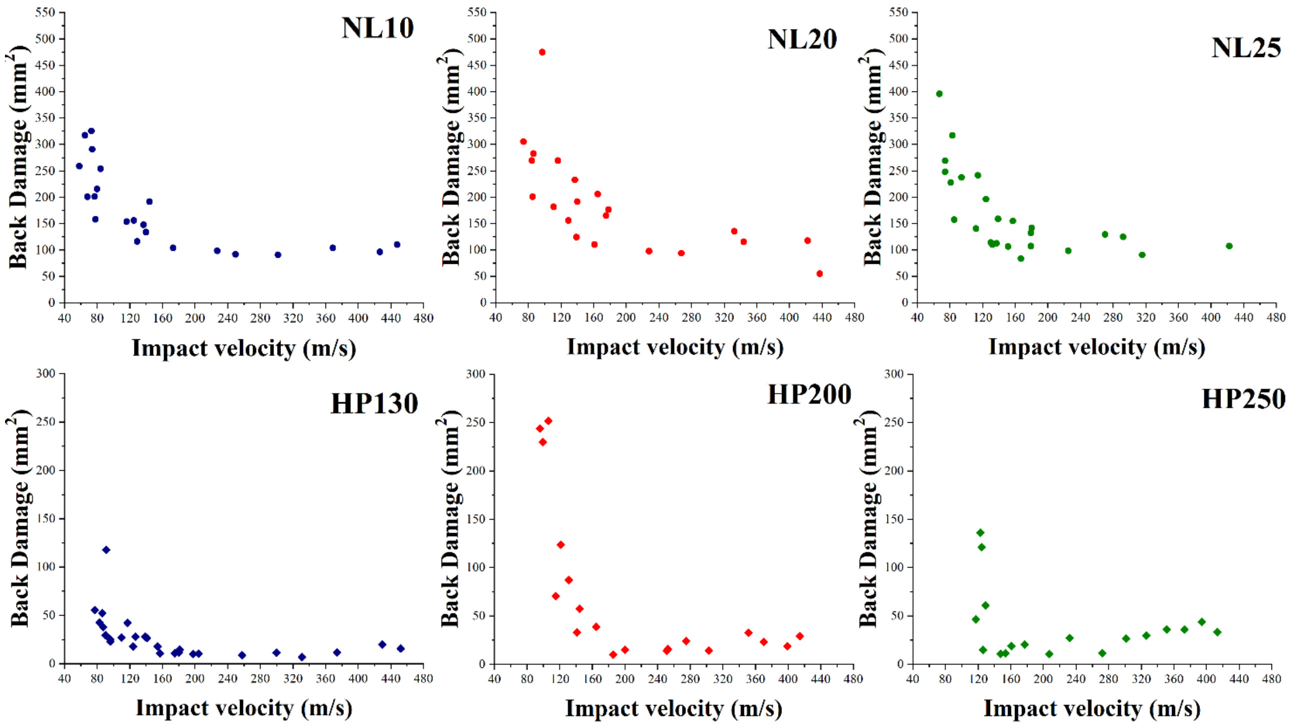

Figure 8: Evolution of back damage area extent as a function of impact velocity for the six core materials

3.2 Skin and Sandwich Structures Ballistic Response

As already shown for core materials, the application of Lambert-Jonas interpolation to the impact and residual velocities data set allowed to evaluate the ballistic limits of the PP and PPC skins and of the six sandwich configurations whose curves are shown in Figure S5 and S6 of Supplementary Materials. Concerning the skins, PP laminates displayed a ballistic limit of 101.16 m/s that is very similar to the 100.34 m/s obtained for the compatibilized PPC. Contrary to what observed by Simeoli et al. [39], by Boccardi et al. [40] and by Sorrentino et al. [41], who disclosed a detrimental effect of coupling agent on the low velocity impact response of polymeric composite laminates due to the improved fiber-matrix interface that makes the material more brittle hindering some energy dissipation mechanisms, no significant effects of coupling agent on skins impact resistance were detected in the present work. This discrepancy can be explained considering the different interaction time between the sample and the impactor in low and high-velocity impacts. Low-velocity impacts are characterized by a millisecond reaction time that allows the sample to deform and react globally whereas ballistic impacts entail a microsecond reaction time that causes a strong localization of the impact and hence of the sample area involved in the process making negligible the improvement effect in fiber-matrix interface provided by the coupling agent.

The ballistic limits of the six sandwich configurations under study are summarized in Table 2. The high-velocity impacts performed on the cores revealed that PVC foams ensure better impact resistance than all agglomerated corks, but the situation changes when the latter are bound to the skins to obtain the complete structure. Their integration between the load-bearing laminates allows to prevent the premature detachment of sample plugs thus allowing to exploit cork damping capabilities. Indeed, HP130 and NL10 structures, which are characterized by the same weight, display comparable ballistic limits especially with PP-based skins, whereas NL25 structures are characterized by a ballistic limit between 5 and 16 m/s higher. For the skins, no significant differences could be observed between PP and PPC and this conclusion is still valid when HP130 structures are considered. The severe localization of the impact assisted by the typical damage mode of the foam and the higher stiffness of the composite provided by the rigid foam, do not allow to detect any difference in PP and PPC sandwich ballistic response. The damage localization experienced by these composites is confirmed by the analysis of the cross section of the samples shown in Figure 9. The situation is slightly different for NL10 and NL25 composites that display a slight increase in the ballistic limit of 6.5 m/s and 10 m/s, respectively, moving from the PPC to the PP configuration.

Table 2: Ballistic limits of the six sandwich structures under study

Sandwich	Ballistic limit (m/s)
PP_NL10	171.6
PPC_NL10	165.1
PP_NL25	187
PPC_NL25	177.6
PP_HP130	171.1
PPC_HP130	172.3

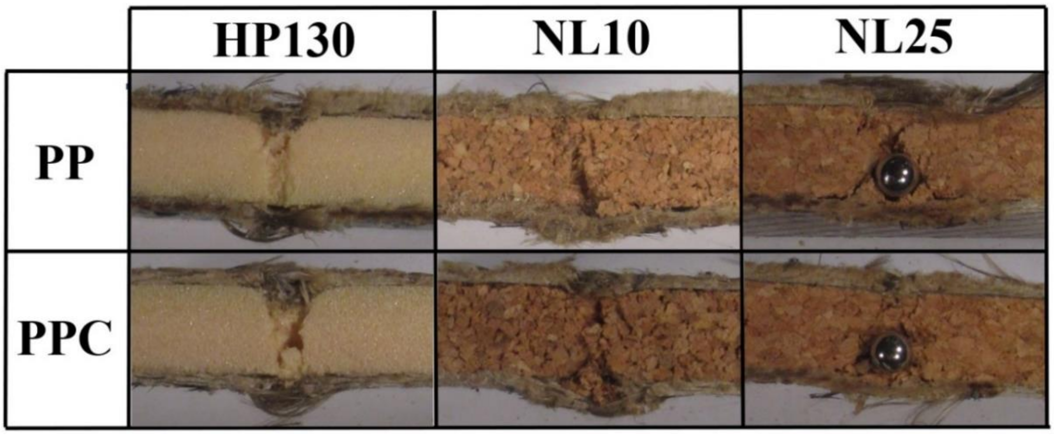

Figure 9: Cross-sections of the six sandwich configurations impacted at 175 m/s which allowed to estimate the damage experienced by the composites

Even if the increment in ballistic limit is minimal, it can be ascribed to the different damage mode of agglomerated cork with respect to the foam. The intergranular fracture that arises in the bio-based core tends to evolve with a conical shape as already acknowledged for the cores and as confirmed by Figure 9. This means that the exit side is characterized by a wider area than the enter side thus increasing progressively the area of the sample interested by the impact especially in correspondence of the ballistic limit. This means that the area of the bottom skin that reacts to the impact may be extended to such an extent to make slightly detectable the negative effect played by the coupling agent.

3.3 Core materials Finite Element Analysis: Results

The finite element simulations were run along the whole impact velocity range investigated with the ballistic experimental campaign and the results obtained for HP130 foam are shown in Figure 10. A perfect fitting between the experimental data and the numerical simulation curve was achieved with a coefficient correlation of 0.999 and an average error, i.e. the mean of the differences between the numerical and the experimental values normalized respect to the experimental values, of 5.87 %. These results prove the feasibility of the CRUSHABLE FOAM model to simulate the impact response of the PVC foams under study.

The comparison between the experimental data and the finite element analysis results of agglomerated cork NL25 is shown in Figure 11. The fitting obtained is not perfect as in the case of the polymeric foam, but it provides satisfying results with a coefficient correlation of 0.997 and an average error of 12.6 % thus confirming the suitability of the CRUSHABLE FOAM model to simulate the ballistic impact response of complex and heterogeneous materials such as agglomerated cork.

In Figure 12 the Von Mises stress distributions for both HP130 (a) and NL25 (d) are reported. The numerical results corroborate the experimental ones in fact the higher stiffness of HP130 determines a strong localization of the damage and a concentration of the reaction forces in the impacted area. Different is agglomerated cork response which thanks to its softer nature, allows a more global response of the specimen despite the localization of the damage. From the damage mode point of view, the finite element simulation is able to reproduce quite faithfully the plugging damage mode which arises in the synthetic foam as shown in Figure 13. From agglomerated cork point of view the situation is more complex in fact the simulation is not able to reproduce the conical fracture that arises in the natural core, but despite this limitation it allows to point out some differences in the damage mode with respect to the PVC foam. In particular, looking at the results for NL25 reported in Figure 14, the simulation is able to capture the detachment of different specimen pieces as actually occurred during the experimental testing of the material.

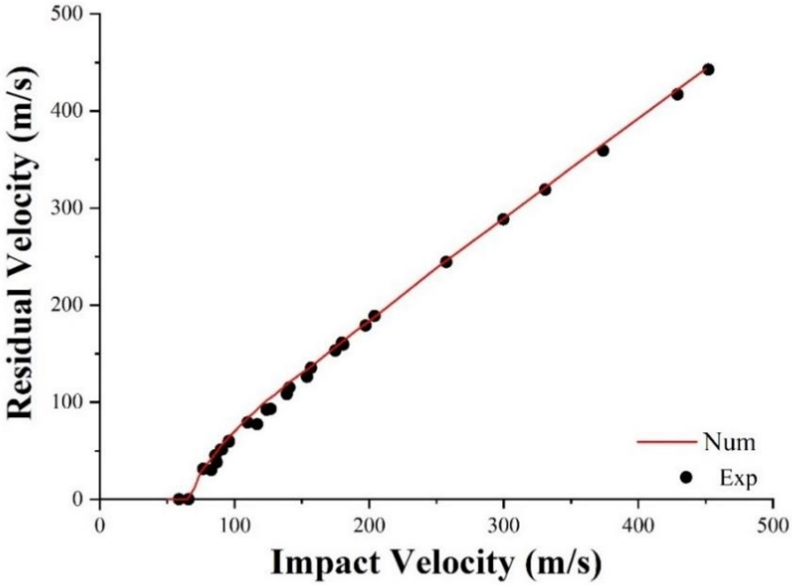

Figure 10: Fitting between the experimental data and the numerical simulation of HP130 PVC foam

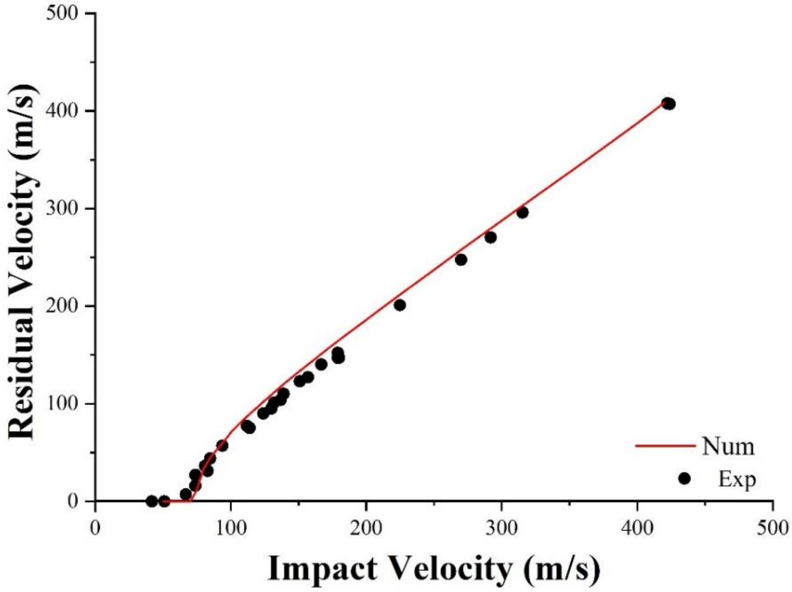

Figure 11: Fitting between the experimental data and the numerical simulation of NL25 agglomerated cork

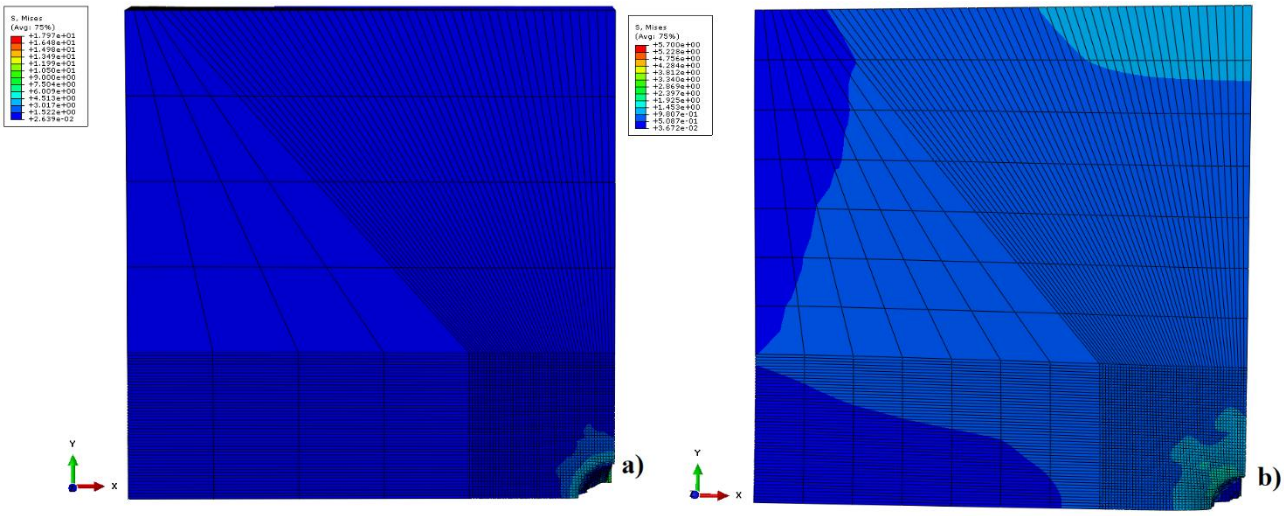

Figure 12: Von Mises stress distributions for HP130 (a) and NL25 (b)

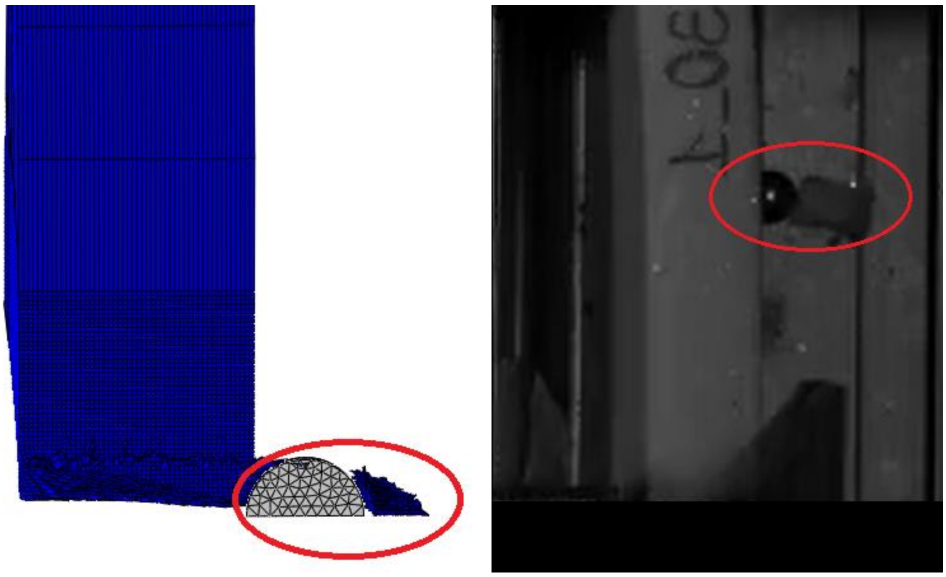

Figure 13: HP130 damage mode numerical v.s. experimental

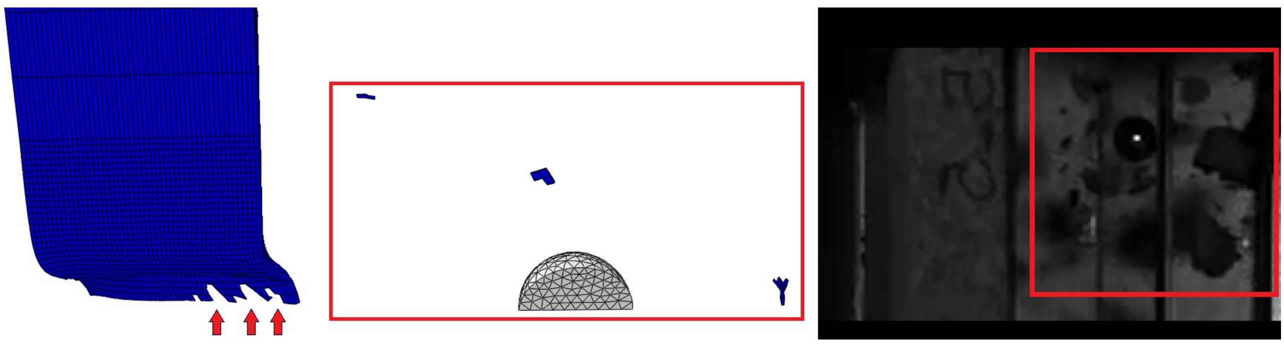

Figure 14: NL25 damage mode numerical v.s. experimental

4 CONCLUSIONS

The present work dealt with the ballistic impact response of agglomerated cork and the resulting bio-based sandwich structures with PP flax/basalt hybrid skins. The experimental campaign carried out on the complete structures and on their single components, i.e. the cores and the skins, and the finite element analysis performed on NL25 agglomerated cork and HP130 PVC foam allowed to draw some important conclusions.

Agglomerated cork ballistic resistance is definitely lower than the one of the synthetic PVC foam employed as benchmark and its ballistic limit does not increase linearly with density, contrary to PVC foam one. Both results are mainly due to the premature detachment of cork plugs induced by the weak interface between cork granules and polymeric binder. This point of weakness acts as a bottle-neck which delimits the upper limit achievable with the bio-based core.

Agglomerated cork and PVC foams are characterized by two different damage modes. Agglomerated cork is characterized by a conoidal intergranular fracture whereas PVC foams display a cylindrical plugging damage mode. Despite the different fracture mechanism, both core types are characterized by a progressive decrease of damage area extent for increasing impact velocities. This is due to a decrease in impact reaction time that prevents sample global reaction and promotes damage localization. This extreme localization of the damage makes also negligible the fiber-matrix interface improvement provided by the maleic anhydride coupling agent to the composite skins.

When embedded between the two skins, agglomerated cork impact performance strongly improves thanks to the hindering of sample plugs detachment thus allowing the full exploitation of cork energy absorption capacities. Indeed, NL10 and HP130 sandwich structures, characterized by the same weight, displayed comparable ballistic limits whereas NL25, which displayed a ballistic limit close to HP130 when employed as core, provided an increase of 15 m/s when employed as core material in the sandwich structure.

The CRUSHABLE FOAM material model in conjunction with the ductile damage criterion, implemented in the finite element analysis software ABAQUS, allowed to perfectly simulate the ballistic impact response of the polymeric PVC foam HP130 and permitted to achieve satisfying results even with agglomerated cork NL25 despite its heterogeneous microstructure. The possibility to successfully simulate the perforation phenomena of cork provides an efficient tool not only for the present work purposes, but also for other sandwich configurations.

The results obtained in this work together with the literature works that demonstrated the improved low-velocity impact crashworthiness of agglomerated cork with respect to other synthetic foams [42,43], allows to conclude that agglomerated cork core is a suitable bio-based alternative to synthetic foams in all those applications where an improved impact resistance is the main design parameter. For example, high and low-velocity impact resistant camper shell could be produced taking advantage of this core material increasing the safety in case of accident or of foreign object debris impact and reducing the waste disposal issues at the end of vehicles life-cycle.

Data availability Statement: The raw/processed data required to reproduce these findings cannot be shared at this time as the data also forms part of an ongoing study.

Author Contributions: Claudia Sergi: Data curation, Formal analysis, Investigation, Methodology, Visualization, Writing – Original draft. **Fabrizio Sarasini**: Methodology, Validation, Writing – Review & Editing. **Pietro Russo**: Methodology, Investigation, Writing – Review & Editing. **Libera Vitiello**: Investigation, Writing – Review & Editing. **Enrique Barbero**: Conceptualization, Methodology, Supervision, Writing – Review & Editing. **Sonia Sanchez-Saez**: Conceptualization, Methodology, Supervision, Writing – Review & Editing. **Jacopo Tirillò:** Conceptualization, Formal analysis, Investigation, Supervision, Validation, Writing – Review & Editing.

REFERENCES

[1] Naik S, Dandagwhal RD, Loharkar PK. A review on various aspects of Kevlar composites used in ballistic applications. Mater Today Proc 2020;21:1366–74. doi:10.1016/j.matpr.2020.01.176.

[2] Cha J, Kim Y, Kumar S, Kumar S, Choi C, Kim C. Ultra-high-molecular-weight polyethylene as a hypervelocity impact shielding material for space structures. Acta Astronaut 2020;168:182–90. doi:10.1016/j.actaastro.2019.12.008.

[3] Nunes LM, Paciornik S, Almeida JRM. Evaluation of the damaged area of glass-fiber-reinforced epoxy-matrix composite materials submitted to ballistic impacts. Compos Sci Technol 2004;64:945–

54. doi:10.1016/S0266-3538(03)00105-2.
[4] da Silva Junior JEL, Paciornik S, Almeida JRMÕ. Evaluation of the effect of the ballistic damaged area on the residual impact strength and tensile stiffness of glass-fabric composite materials. Compos Struct 2004;64:123–7. doi:10.1016/S0263-8223(03)00220-4.
[5] Kaboglu C, Yu L, Mohagheghian I, Blackman BRK, Kinloch AJ, Dear JP. Effects of the core density on the quasi-static flexural and ballistic performance of fibre-composite skin / foam- core sandwich structures. J Mater Sci 2018;53:16393–414. doi:10.1007/s10853-018-2799-x.
[6] Mahesh C, Nair RP. Numerical Research on the Effect of Impactor Shape and Core Characteristics on the Ballistic Impact Response of Marine Sandwich Composite Plates. Int J Recent Technol Eng 2019;8:1236–40. doi:10.35940/ijrte.B1231.0782S319.
[7] Ahmadi H, Liaghat G. Analytical and Experimental Investigation of High Velocity Impact on Foam Core Sandwich Panel. Polym Compos 2019. doi:10.1002/pc.25034.
[8] Zhao N, Ye R, Tian A. Experimental and numerical investigation on the anti-penetration performance of metallic sandwich plates for marine applications. J Sandw Struct Mater 2020;22:494–522. doi:10.1177/1099636219855335.
[9] Abbasi M, Nia AA. High-velocity impact behavior of sandwich structures with AL faces and foam cores — Experimental and numerical study. Aerosp Sci Technol 2020;105:106039. doi:10.1016/j.ast.2020.106039.
[10] Aryal B, Morozov E V, Shankar K. Effects of ballistic impact damage on mechanical behaviour of composite honeycomb sandwich panels. J Sandw Struct Mater 2020;0:1–22. doi:10.1177/1099636220909743.
[11] Wang Y, Yu Y, Wang C, Zhou G, Karamoozian A, Zhao W. On the out-of-plane ballistic performances of hexagonal , reentrant , square , triangular and circular honeycomb panels. Int J Mech Sci 2020;173. doi:10.1016/j.ijmecsci.2019.105402.
[12] Santos da Luz F, da Costa Garcia Filho F, Oliveira MS, Cassiano Nascimento LF, Monteiro SN. Composites with Natural Fibers and Conventional Materials Applied in a Hard Armor : A Comparison. Polymers (Basel) 2020;12:1–13. doi:10.3390/polym12091920.
[13] Jover N, Shafiq B, Vaidya U. Ballistic impact analysis of balsa core sandwich composites. Compos PART B 2014;67:160–9. doi:10.1016/j.compositesb.2014.07.002.
[14] Sanchez-Saez S, García-Castillo SK, Barbero E, Cirne J. Dynamic crushing behaviour of agglomerated cork. Mater Des 2015;65:743–8. doi:10.1016/j.matdes.2014.09.054.
[15] Jardin RT, Fernandes FAO, Pereira AB, Alves de Sousa RJ. Static and dynamic mechanical response of different cork agglomerates. Mater Des 2015;68:121–6. doi:10.1016/j.matdes.2014.12.016.
[16] Gómez A, Sanchez-Saez S, Barbero E. Compression impact behaviour of agglomerated cork at intermediate strain rates. Eur J Wood Wood Prod 2021. doi:10.1007/s00107-020-01638-2.
[17] Ptak M, Kaczynski P, Fernandes FAO, Alves de Sousa RJ. Assessing impact velocity and temperature effects on crashworthiness properties of cork material. Int J Impact Eng 2017;106:238–48. doi:10.1016/j.ijimpeng.2017.04.014.
[18] Kaczynski P, Ptak M, Wilhelm J, Fernandes FAO, Alves De Sousa RJ. High-energy impact testing of agglomerated cork at extremely low and high temperatures. Int J Impact Eng 2019;126:109–16. doi:10.1016/j.ijimpeng.2018.12.001.
[19] Kaczynski P, Ptak M, Fernandes FAO, Chybowski L, Wilhelm J, Alves de Sousa RJ. Development and Testing of Advanced Cork Composite Sandwiches for Energy-Absorbing Structures. Materials (Basel) 2019;12. doi:10.3390/ma12050697.
[20] Sanchez-Saez S, Barbero E, Garcia-Castillo SK, Ivañez I, Cirne J. Experimental response of agglomerated cork under multi-impact loads. Mater Lett 2015;160:327–30. doi:10.1016/j.matlet.2015.08.012.
[21] Wang H, Ramakrishnan KR, Shankar K. Experimental study of the medium velocity impact response of sandwich panels with different cores. JMADE 2016;99:68–82. doi:10.1016/j.matdes.2016.03.048.
[22] Arteiro A, Reis ALMA, Nóvoa PJRO, Silva LFM, Zupan M, Marques AT. Low velocity impact and flexural performance of sandwich structures with cork and polymer foam cores. Cienc e Tecnol Dos Mater 2013;25:79–84. doi:10.1016/j.ctmat.2014.03.003.
[23] Sarasini F, Tirillò J, Lampani L, Sasso M, Mancini E, Burgstaller C, et al. Static and dynamic characterization of agglomerated cork and related sandwich structures. Compos Struct 2019;212:439–51. doi:10.1016/j.compstruct.2019.01.054.

[24] Boria S, Raponi E, Sarasini F, Tirillò J, Lampani L. Green sandwich structures under impact : experimental vs numerical analysis. Procedia Struct Integr 2018;12:317–29. doi:10.1016/j.prostr.2018.11.084.
[25] Sanchez-Saez S, Barbero E, Cirne J. Experimental study of agglomerated-cork-cored structures subjected to ballistic impacts. Mater Lett 2011;65:2152–4. doi:10.1016/j.matlet.2011.04.083.
[26] Sarasini F, Tirillò J, Lampani L, Barbero E, Sanchez-Saez S, Valente T, et al. Impact behavior of sandwich structures made of flax / epoxy face sheets and agglomerated cork. J Nat Fibers 2020;17:168–88. doi:10.1080/15440478.2018.1477084.
[27] Ivañez I, Sánchez-saez S, Garcia-castillo SK, Barbero E, Amaro A, Reis PNB. High-velocity impact behaviour of damaged sandwich plates with agglomerated cork core. Compos Struct 2020;248. doi:10.1016/j.compstruct.2020.112520.
[28] Fernandes FAO, Pascoal RJS, Sousa RJA De. Modelling impact response of agglomerated cork. J Mater 2014;58:499–507. doi:10.1016/j.matdes.2014.02.011.
[29] Ben-Dor G, Dubinsky A, Elperin T. On the Lambert – Jonas approximation for ballistic impact. Mech Res Commun 2002;29:137–9. doi:10.1016/S0093-6413(02)00246-X.
[30] Carranza I, Crocombe AD, Mohagheghian I, Smith PA, Sordon A, Meeks G, et al. Characterising and modelling the mechanical behaviour of polymeric foams under complex loading. J Mater Sci 2019;54:11328–44. doi:10.1007/s10853-019-03673-8.
[31] Ozturk EU, Anlas G. Finite element analysis of expanded polystyrene foam under multiple compressive loading and unloading. Mater Des 2011;32:773–80. doi:10.1016/j.matdes.2010.07.025.
[32] Chessin N, Driver WE. Compression and Friction Properties of Rigid Polyurethane Foams. J Cell Plast 1967:185–91.
[33] Lakes R. Foam Structures with a Negative Poisson's Ratio. Science (80-) 1987;235:1038–40.
[34] Tita V, Caliri Junior MF. Numerical simulation of anisotropic polymeric foams. Lat Am J Solids Struct · 2012;1:1–21. doi:10.1590/S1679-78252012000200005.
[35] Pereira H. The rationale behind cork properties: A review of structure and chemistry. BioResources 2015;10:1–23. doi:10.15376/biores.10.3.Pereira.
[36] Buitrago BL, García-castillo SK, Barbero E. Experimental analysis of perforation of glass / polyester structures subjected to high-velocity impact. Mater Lett 2010;64:1052–4. doi:10.1016/j.matlet.2010.02.007.
[37] Lopez-Puente J, Zaera R, Navarro C. Experimental and numerical analysis of normal and oblique ballistic impacts on thin carbon / epoxy woven laminates. Compos Part A 2008;39:374–87. doi:10.1016/j.compositesa.2007.10.004.
[38] Amaro AM, Balbis Reis NP, Ivañez I, Sanchez-Saez S, Garcia-castillo SK, Barbero E. The High-Velocity Impact Behaviour of Kevlar Composite Laminates Filled with Cork Powder. Appl Sci 2020;10. doi:10.3390/app10176108.
[39] Simeoli G, Sorrentino L, Touchard F, Mellier D, Oliviero M, Russo P. Comparison of falling dart and Charpy impacts performances of compatibilized and not compatibilized polypropylene / woven glass fibres composites. Compos Part B 2019;165:102–8. doi:10.1016/j.compositesb.2018.11.090.
[40] Boccardi S, Meola C, Carlomagno GM, Sorrentino L, Simeoli G, Russo P. Effects of interface strength gradation on impact damage mechanisms in polypropylene / woven glass fabric composites. Compos Part B 2016;90:179–87. doi:10.1016/j.compositesb.2015.12.004.
[41] Sorrentino L, Simeoli G, Iannace S, Russo P. Mechanical performance optimization through interface strength gradation in PP / glass fi bre reinforced composites. Compos Part B 2015;76:201–8. doi:10.1016/j.compositesb.2015.02.026.
[42] Castro O, Silva JM, Devezas T, Silva A, Gil L. Cork agglomerates as an ideal core material in lightweight structures. Mater Des 2010;31:425–32. doi:10.1016/j.matdes.2009.05.039.
[43] Barbosa AQ, Silva LFM, Öchsner A, Silva LFM, Hygrothermal AÖ. Hygrothermal aging of an adhesive reinforced with microparticles of cork. J Adhes Sci Technol 2015;4243:1–19. doi:10.1080/01694243.2015.1041358.